Cell and Tissue Research (2019) 376:83–96
https://doi.org/10.1007/s00441-018-2949-0

REGULAR ARTICLE

Distribution of FMRFamide-related peptides and co-localization with glutamate in *Cupiennius salei*, an invertebrate model system

Emily A. Tarr[1] · Brian M. Fidler[1] · Kyrstin E. Gee[1] · Carly M. Anderson[1] · Anna K. Jager[1] · Neil M. Gallagher[1] · Kaelyn P. Carroll[1] · Ruth Fabian-Fine[1]

Received: 22 June 2018 / Accepted: 9 October 2018 / Published online: 8 November 2018

Abstract

FMRFamide-related proteins have been described in both vertebrate and invertebrate nervous systems and have been suggested to play important roles in a variety of physiological processes. One proposed function is the modulation of signal transduction in mechanosensory neurons and their associated behavioral pathways in the Central American wandering spider *Cupiennius salei*; however, little is known about the distribution and abundance of FMRFamide-related proteins (FaRPs) within this invertebrate system. We employ immunohistochemistry, Hoechst nuclear stain and confocal microscopy of serial sections to detect, characterize and quantify FMRFamide-like immunoreactive neurons throughout all ganglia of the spider brain and along leg muscle. Within the different ganglia, between 3.4 and 12.6% of neurons showed immunolabeling. Among the immunoreactive cells, weakly and strongly labeled neurons could be distinguished. Between 71.4 and 81.7% of labeled neurons showed weak labeling, with 18.3 to 28.6% displaying strong labeling intensity. Among the weakly labeled neurons were characteristic motor neurons that have previously been shown to express ɣ-aminobutyric acid or glutamate. Ultrastructural investigations of neuromuscular junctions revealed mixed presynaptic vesicle populations including large electron-dense vesicles characteristic of neuropeptides. Double labeling for glutamate and FaRPs indicated that a subpopulation of neurons may co-express both neuroactive compounds. Our findings suggest that FaRPs are expressed throughout all ganglia and that different neurons have different expression levels. We conclude that FaRPs are likely utilized as neuromodulators in roughly 8% of neurons in the spider nervous system and that the main transmitter in a subpopulation of these neurons is likely glutamate.

Keywords Spider central nervous system · Synaptic circuits · Co-transmission · Neuromuscular junctions · Neuropeptides

Introduction

Over the past three decades, the phenomenon of co-transmission and co-release of two or more transmitters from individual neurons has become well established in both vertebrate and invertebrate nervous systems. Co-expression of two counteracting small molecule transmitters has been described in both vertebrate and invertebrate systems (Schwarzer and Sperk 1995; Sloviter et al. 1996; Fabian-Fine et al. 2015). However, a majority of cases where co-transmission has been described involve fast-acting, small molecule transmitters in combination with one or more neuropeptides that are released in a frequency-dependent manner (Jan and Jan 1982; Whim and Lloyd 1989; Loi and Tublitz 2000; Liu et al. 2011; van den Pol 2012; Nässel 2018).

Four important aspects of co-transmission are as follows: (1) the importance of co-transmission in the context of behavior and synaptic plasticity (Whim and Lloyd 1989; Loi and Tublitz 2000; Sloviter et al. 1996); (2) the diversity of functional characteristics in which co-transmission is utilized (Jan and Jan 1982; Whim and Lloyd 1989; Sloviter et al. 1996); (3) the importance to identify the co-transmitted neuroactive compounds and their receptors within individual neurons to conduct functional studies; and (4) the importance of intact neuronal networks and synaptic circuits for functional studies. To this end, invertebrate model systems have proven particularly advantageous. These systems often provide comparatively easy access to intact synaptic circuits, contain large

Emily A. Tarr and Brian M. Fidler contributed equally to this work.

✉ Ruth Fabian-Fine
rfabianfine@smcvt.edu

[1] Department of Biology, Saint Michael's College, One Winooski Park, Box 283, Colchester, VT, USA

individually identifiable neurons that are suitable for intracellular recordings and contain a limited number of cells within the synaptic circuits.

One exceptionally suitable model system to study co-transmission are the mechanosensory neurons in the walking legs of the Central American wandering spider *Cupiennius salei*. In these neurons, co-transmission is utilized in efferent neurons that exert central control onto mechanosensory neurons (Fabian-Fine et al. 1999b, 2000). The mammalian equivalent to this invertebrate system are the vestibular and cochlear systems, in which mechanosensory hair cells and adjacent afferent neurons receive efferent innervation (Schrott-Fischer et al. 2007; Rabbitt and Brownell 2011). The bony encasement of the cochlear and vestibular systems makes the examination of the mammalian systems more challenging compared to the peripherally located invertebrate equivalents. Numerous similarities in the efferent innervation of mechanosensory neurons in both the invertebrate and vertebrate systems underline the possibility of a common ancient origin; however, it is currently unclear whether these systems are homologous or analogous. Biochemical, morphological and functional studies on intact synaptic circuits of this invertebrate model system are thus important and of relevance.

Walking legs of wandering spiders contain numerous mechanosensory hair and slit sensilla that are innervated by large, bipolar mechanosensory neurons (Foelix and Chu-Wang 1973; Barth and Libera 1970; Seyfarth and French 1994; Fabian-Fine et al. 1999b, Fabian-Fine et al. 2000). The dendrites, somata and initial axon segments of these peripherally located mechanosensory neurons are innervated by a multitude of morphologically and biochemically diverse efferent fibers (Fabian-Fine et al. 1999b, 2000; Widmer et al. 2005; Fabian-Fine et al. 2017). These fibers have been shown to exert inhibitory and excitatory functions onto the sensory neurons (Panek et al. 2002; Panek and Torkkeli 2005; Widmer et al. 2005; Pfeiffer et al. 2009). Extensive ultrastructural and immunohistochemical investigations have revealed that numerous efferent synapses are likely co-releasing two or more transmitters/modulators from individual synapses. The presence of large electron-dense vesicles, which is characteristic of neuropeptides (Salio et al. 2006; Merighi et al. 2011; van den Pol 2012), suggests that neuropeptides are likely playing a prominent role in the efferent control of mechanosensory signal transduction. We recently demonstrated that neuropeptide candidates within these synapses are FMRFamide-related peptides (FaRPs; Fabian-Fine et al. 2017). Over recent years, FaRPs have been shown to act as neuromodulators in a number of different invertebrate systems. One example is the excitatory action of FaRPs in chromatophore neuromuscular junctions of the cuttlefish *Sepia officinalis* (Loi and Tublitz 2000, see discussion). In auxiliary hearts of mosquitoes that propel hemolymph into the antennae of the insects, FaRPs have accelerating effects (Suggs et al. 2016). Although the presence of FaRPs has been described in the visual system and along mechanosensory neurons of *C. salei* (Becherer and Schmid 1999; Fabian-Fine et al. 2017), the distribution of these neuropeptides throughout the rest of the spider nervous system has not been described in detail. For future functional studies, this knowledge is of crucial importance, which is why we investigate the detailed distribution of FMRF-like immunoreactive (FMRFa-LIR) neurons in all areas of the spider CNS and along leg muscle.

Materials and methods

Experimental animals

All experiments were performed on adult females of the Central American wandering spider *Cupiennius salei*. Animals were bred in the laboratory, raised individually in plastic containers and fed with juvenile or adult crickets. Animals were kept under normal environmental conditions with natural day/light cycles at 23 °C.

Tissue dissection

Prior to dissection, spiders were deeply anesthetized with CO_2. After removal of the distal leg segments below the patella, animals were perfused with paraforaldehyede (PFA) consisting of 6% paraformaldehyde in 0.1 M phosphate-buffered saline pH 7.4 (PBS). The proximal leg segments and the prosoma containing the CNS of the animals were submerged in 6% PFA and kept in the refrigerator overnight. Dissection of leg muscles and CNS tissue was carried out in PBS as described previously (Fabian-Fine et al. 2015). The CNS was embedded in 4% agarose (Sigma-Aldrich A9539) and sectioned using a Leica VT 1000S vibrating microtome at a thickness of 70 μm. Individual brain slices were transferred into 16-well dishes containing PBS using a fine paintbrush.

Immunohistochemistry

Anti-FMRFamide immunolabeling of CNS tissue Brain sections were washed in PBS (3 × 20 min) and incubated in permeabilization and blocking medium (PBM) consisting of 0.05% Triton-X 100 (Sigma X100), 10% normal goat serum (Sigma G9023) and 0.25% bovine serum albumin (Sigma A4503) for 15 min to permeabilize the cell membranes and prevent unspecific cross-reaction of the primary antiserum. The polyclonal antiserum against FaRPs was the same used in our previous studies (Fabian-Fine et al. 2017; rabbit anti-FMRFamide Sigma Millipore AB15348) and was diluted 1:1000 in PBS containing 10% PBM for 24 h at 6 °C. During the first and final 2 h of primary antiserum incubation, brain slices were placed on a shaker and gently agitated on ice

to ensure a homogenous penetration of the antiserum. Prior to incubation with the secondary antibody, brain slices were washed in PBS (4 × 20 min on ice) and incubated in PBM (15 min). The secondary Cy3-conjugated goat-anti-rabbit antibody (Jackson ImmunoResearch Laboratories 111-165-003) was used at a dilution of 1:500 in PBS containing 10% PBM; the tissue was immersed in the antibody solution for 24 h at 6 °C. The brain slices were washed in PBS (3 × 10 min) and incubated in Hoechst Blue (Sigma H 6024) at a concentration of 1:3000 in PBS for 20 min on ice to stain neuronal nuclei. After additional washing in PBS (3 × 10 min), brain slices were mounted on glass slides using Mowiol (Sigma-Aldrich 81381; Fabian-Fine et al. 2015). To minimize bleaching, the preparations were left to polymerize overnight at 6 °C.

FMRFamide immunolabeling of muscle tissue Incubation with the polyclonal anti-FMRFamide antiserum was carried out identically to FMRFamide immunolabeling of the brain slices with the exception that muscle tissue was not embedded in agarose or vibratome sectioned. Immunolabeled muscle fibers were mounted in Mowiol on glass slides.

FMRFamide-glutamate double labeling Animals were perfused, dissected and immunolabeled as described above with the following exceptions. The fixative used contained 4% PFA and 0.15% glutaraldehyde in 0.1 M PBS pH 7.4. The primary antiserum solution was used at a dilution of 1:800 for both the polyclonal anti-FMRFamide antiserum (Rabbit anti-FMRFamide Sigma Millipore AB15348) and the mouse anti-glutamate antibody (Sigma-Aldrich G9282). The secondary antibodies (Cy3 goat-anti-rabbit Jackson ImmunoResearch no. 111-165-003; Alexa 488 goat-anti-mouse Jackson ImmunoResearch no. 115-545-146) were diluted 1:500 in PBS containing 10% PBM. Incubation of the tissue followed for 24 h at 6 °C. After subsequent washing in PBS (3 × 10 min), the tissue was stained with Hoechst nuclear stain as described above. Preparations were washed in PBS (5 × 10 min) before mounting in Mowiol on glass slides. Slides were left overnight at 6 °C to allow polymerization of the embedding medium prior to examination with a Zeiss LSM 510 confocal microscope.

Electron microscopy Preparations intended for EM analysis were processed as described previously (Fabian-Fine et al. 2015). In brief, 2.5% glutaraldehyde and 4% PFA in 0.1 M PBS, pH 7.4 was used for fixation overnight at 6 °C. Preparations were osmicated for 15 min in 0.5% OsO_4-PBS prior to dehydration with molecular-grade ethanol and propylene oxide. The tissue was embedded in Araldite (Electron Microscopy Sciences 13900) and polymerized at 60 °C overnight. Series of 60-nm ultrathin sections were cut with a Leica Ultracut EM UC7 and collected on Pioloform-coated single-slot copper grids. After contrasting with uranyl acetate (5 min) and Reynold's lead citrate (5 min), examination was carried out using a FEI Tecnai 12 electron microscope operated at 80 kV.

Antibody/antiserum characterization Preparations treated with the secondary antibodies only lacked immunofluorescence demonstrating that immunofluorescence was not due to non-specific cross-reaction of the secondary antibodies. The specificity of the Sigma anti-glutamate antibody in spider tissue has been tested and discussed previously using double labeling for glutamate and the vesicular glutamate transporter, which both appeared co-localized within the same neurons (Fabian-Fine et al. 2015). The anti-FMRFamide antiserum has also been used in spider tissue. We analyzed the transcriptomes of *C. salei* and identified at least two FMRFamide-like peptides (accession numbers KY074554 and KY07455) that are likely recognized by this antiserum (Fabian-Fine et al. 2017). The specificity of antibody binding is also supported by the FMRFamide distribution pattern throughout the visual system in *C. salei* that has been described previously (Becherer and Schmid 1999) and matches our observations described here.

Image acquisition

Digital image acquisition and analysis were carried out using a Zeiss 510 Meta laser-scanning microscope with × 10/0.3, × 20/0.75, × 40/1.3 Plan-Neofluar, × 63/1.4 oil Plan-apochromat objectives. For image analysis, the Zeiss ZEN 2012 laser scanning microscope software and Adobe Photoshop and Illustrator were used.

Quantitative image analysis A total of 213 confocal images through the CNS were utilized for quantitative analysis. Only images that were representative of the typical labeling pattern were chosen for evaluation. The numbers of evaluated images per ganglion were as follows: pedipalpal $n = 45$ (n, number of confocal image series evaluated); opisthosomal $n = 25$; walking legs $n = 49$; cheliceral, $n = 54$; posterior cell layer, $n = 29$; dorsal cell layer, $n = 11$). Each confocal image consisted of 5–20 individual 1–3-μm-thick optical sections. To distinguish neurons from glia cells, we utilized the characteristic shapes of the nuclei. The round, Hoechst Blue–stained neuronal nuclei could be easily distinguished from the elliptical and more brightly stained nuclei characteristic of glia cells within this tissue (for details, see Fabian-Fine et al. 2015). Individual optical sections were exported as JPEG or TIFF files. Using Adobe Photoshop CS5, the confocal image was reconstructed in numerical order according to the original Z-stack of optical sections. Each optical section was represented as a layer in one file. Neuronal nuclei on each optical section were counted manually on a new layer using the paintbrush tool. Based on the size of the neuronal

nuclei (small, medium, large) and the labeling pattern within the evaluated neurons, we distinguished between unlabeled and labeled neurons. Among the labeled neuron population, strongly and weakly labeled small, medium and large neurons were distinguished with soma sizes ranging from 5 to 24 μm, 15 to 40 μm and 30 to 100 μm, respectively (Fabian-Fine et al. 2015). The first counted layer was moved to the second optical section and a new layer was created to count additional neuronal nuclei that appeared in the second optical section. To ensure that each neuron was only counted once, the first two counted layers were transferred to the third optical section and a new layer was created to count additional neuronal nuclei that appeared in the third optical section. This pattern continued for the remaining optical slices. All data were recorded and graphed using Microsoft Excel. For each ganglion, the total number of counted neurons was used to determine the ratio of labeled versus unlabeled neurons. Ratios of weakly and strongly labeled FMRF-IR neurons and their respective sizes were determined based on the total number of labeled neurons.

Results

Anatomy of the sub- and supraesophageal complexes of the spider CNS and neuron types

The fused spider nervous system is located in the prosoma of the animals (Fig. 1a) and consists of two main complexes, the dorsally located supraesophageal complex and the ventrally located subesophageal complex. The esophagus penetrates through the CNS from anterior to posterior between these two complexes. Each hemisphere of the subesophageal complex consists of four leg ganglia, one anterior pedipalpal ganglion, and one posterior opisthosomal ganglion (Fig. 1b). The supraesophageal complex contains the cheliceral and visual ganglia. As previously described, the neurons in all ganglia differ widely with regard to the size of their somata and nuclei (Babu and Barth 1984; Fabian-Fine et al. 2015). The soma diameters of large neurons range from 30 to 100 μm (mean 46 μm), with an average nuclear size of about 18 μm. Medium-sized neurons are between 15 and 40 μm in diameter (mean 24 μm) with nuclear diameters around 10 μm. The somata of small neurons differ between 5 and 24 μm in diameter (mean 13 μm) with nuclear diameters of 4 μm. The large neurons are presumed motor neurons whereas the medium and small neurons are likely interneurons and globuli cells (Babu and Barth 1984).

FMRFamide-like immunolabeling in walking leg ganglia We observed FMRFa-LIR neurons of all abovementioned sizes throughout all leg ganglia. The labeling pattern within individual neurons varied from weak punctate labeling to strongly labeled neurons that appeared solidly labeled (Fig. 1c–e). Quantitative analysis revealed that 12.6% ($n = 293$) of all observed neurons ($n = 2328$) were labeled (Fig. 2a). The remaining 87.4% ($n = 2035$) of unlabeled somata were identified by their characteristic Hoechst Blue–stained nuclei (Fig. 1e; Fabian-Fine et al. 2015). The majority of labeled neurons showed weak punctate labeling (75.1% $n = 220$); only 24.9% ($n = 73$) displayed strong labeling (Fig. 2b–e). Large motor neurons in the medial areas of each walking leg showed either weak or no labeling (Fig. 1d). High-magnification confocal microscopy demonstrates the granular nature of the immunolabeled epitopes in both strongly and weakly labeled neurons (Fig. 1d and e). Due to the higher density of labeled epitopes, the strongly labeled neurons appeared solidly labeled at lower magnification whereas the signal in weakly labeled neurons appeared punctate. Clearly visible nuclei within the weakly labeled FMRFa-LIR neurons confirmed that weak labeling intensities were not caused by eccentric section planes through the periphery of the neurons. In the leg ganglia, 51.2% ($n = 150$) of labeled neurons were small and weakly labeled; 13.3% ($n = 39$) were medium and weakly labeled; and 10.6% ($n = 31$) were large putative motor neurons (Fig. 3). The percentages of strongly labeled small and medium neurons were 9.2% ($n = 27$) and 15.7% ($n = 46$), respectively. No strongly labeled motor neurons were observed in the leg ganglia (Fig. 3e–h).

FMRFamide-like immunolabeling in opisthosomal ganglia The number of FMRFa-LIR neurons in the opisthosomal ganglia was the second largest relative to the rest of the brain. The percentage of labeled versus unlabeled neurons was 10.2% ($n = 293$) to 89.8% ($n = 2578$), respectively (Fig. 2a). The number of weakly labeled (79.2% $n = 232$) compared to strongly labeled neurons (20.8% $n = 61$) was similar to the predominantly weakly labeled neurons in the leg ganglia (Figs. 2e, 4). Characteristic medium and large neurons on the medial (Fig. 4b) and posterior dorsolateral sides of both ganglia were consistently strongly labeled (Fig. 4d). Among the strongly labeled neurons, 8.9% ($n = 26$) were small, 8.5% ($n = 25$) were medium and 3.4% ($n = 10$) were large (Fig. 3). Numerous immunoreactive axonal projections were observed projecting toward the leg ganglia and into the opisthosomal nerve.

FMRFamide-like immunolabeling in pedipalpal ganglia Of all observed neurons, 8.1% were labeled ($n = 234$) with 91.9% ($n = 2651$) unlabeled (Fig. 2). A majority of labeled neurons were located in the medial and anterolateral regions showing predominantly weak labeling intensities (71.4%; $n = 167$; Figs. 2 and 5). Among the weakly labeled neurons, 26.5% ($n = 62$) were small, 29.5% ($n = 69$) medium and 15.4% ($n = 36$) large. Strongly labeled neurons were observed in both the medial and peripheral areas of the ganglia (Fig. 2a). Only

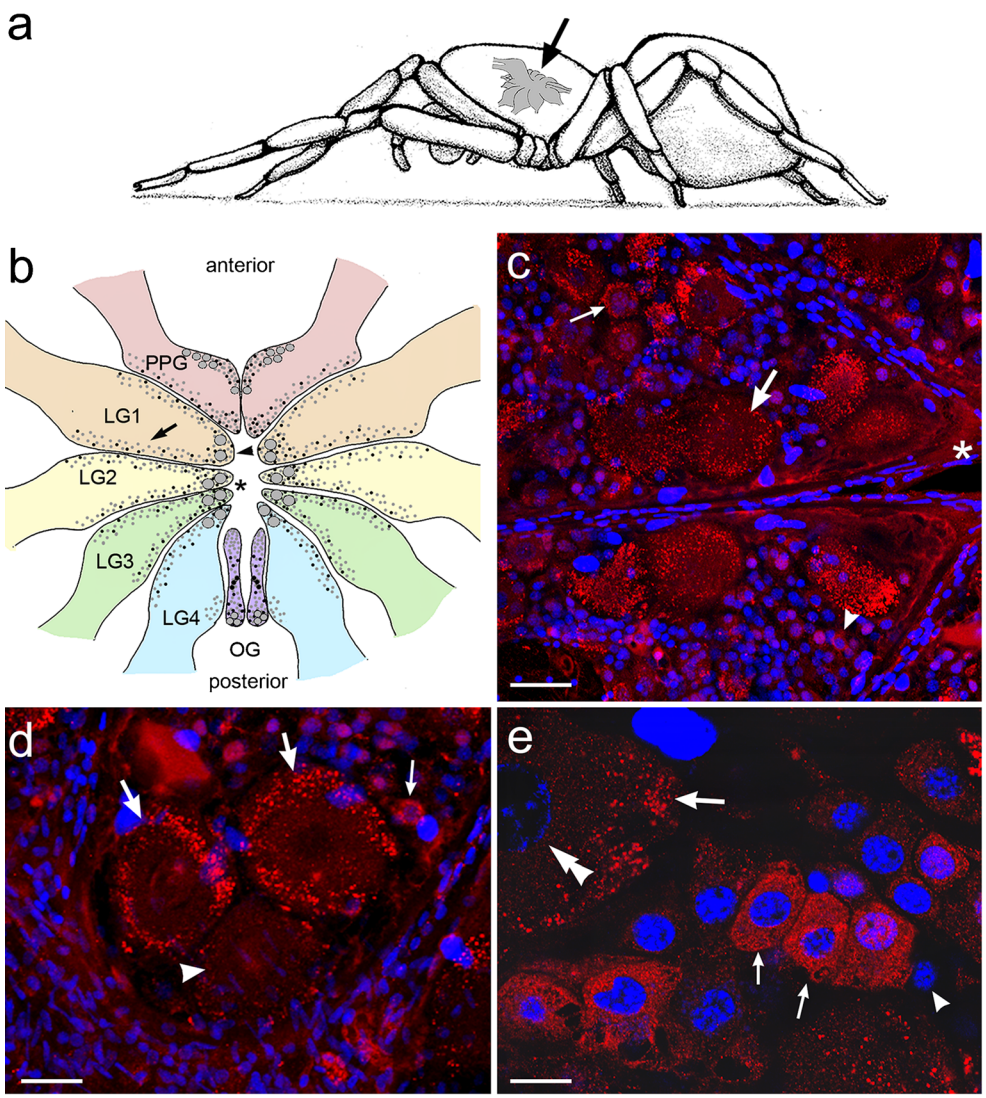

Fig. 1 **a** Schematic drawing of *C. salei.* The fused central nervous system is located in the prosoma of the animals (*arrow*). **b–e** Distribution of FMRFa-LIR (*red*) and Hoechst Blue–stained (*blue*) neurons in the leg ganglia of *C. salei*. **b** Schematic drawing showing the distribution of strongly labeled (*black dots*) and weakly labeled (*gray dots*) FMRFa-LIR neurons in the leg ganglia of all four walking legs (*LG1–LG4*), the pedipalpal ganglia (*PPG*) and opisthosomal ganglia (*OG*) in the left and right hemispheres. Within the *LG*'s, the majority of neurons was observed in the medial (*arrowhead*) and lateral areas (*arrow*). **c** Confocal image of the medial area of walking legs (*asterisks in a and b are corresponding areas*) with large (*large arrow*), medium (*small arrow*) and small (*arrowhead*) weakly labeled neurons. **d** Medial area with two weakly labeled motor neurons (*large arrows*) and one unlabeled motor neuron (*arrowhead*); *small arrow*, strongly labeled small neuron. **e** Higher magnification of small, strongly labeled neurons (*small arrows*), a weakly labeled motor neuron reveals the vesicular nature of the labeling (*large arrow*). *Arrowhead*, unlabeled neuron in which only the nucleic stain is visible. *Double arrowheads*, comparatively faint Hoechst Blue–stained large nucleus in a motor neuron. *Scale bars* (**b**, **c**) 70 μm; (**d**, **e**) 20 μm

28.6% ($n = 67$) of the labeled neurons displayed strong immunoreactivity (19.7% small, 5.6% medium and 3.4% large; Figs. 3 and 4).

Cheliceral ganglia Quantitative analysis revealed that 91.4% ($n = 2792$) of all observed neurons in the cheliceral ganglia were unlabeled with 8.6% ($n = 262$) of labeled neurons. Among the labeled neurons, the majority displayed weak labeling (72.1%; $n = 189$). Strongly labeled neurons accounted for 27.9% ($n = 73$; Figs. 2, 6). Large, putative motor neurons in the anteromedial and anterolateral regions showed weak labeling intensity (Fig. 6a). Small populations of medium-sized neurons in the anteromedial area showed strong (2.7%; $n = 7$) and weak (1.5%; $n = 4$; Fig. 3) labeling intensity (Fig. 6). Similar to the neuropil regions in the other ganglia, numerous FMRFa-LIR varicose fibers of different sizes (small, medium, large) were observed in the cheliceral region (Fig. 6h).

Posterior cell layer (PCL) This ganglion is located posteriorly to the central body (Fig. 7) and contained 3.4% ($n = 153$) of

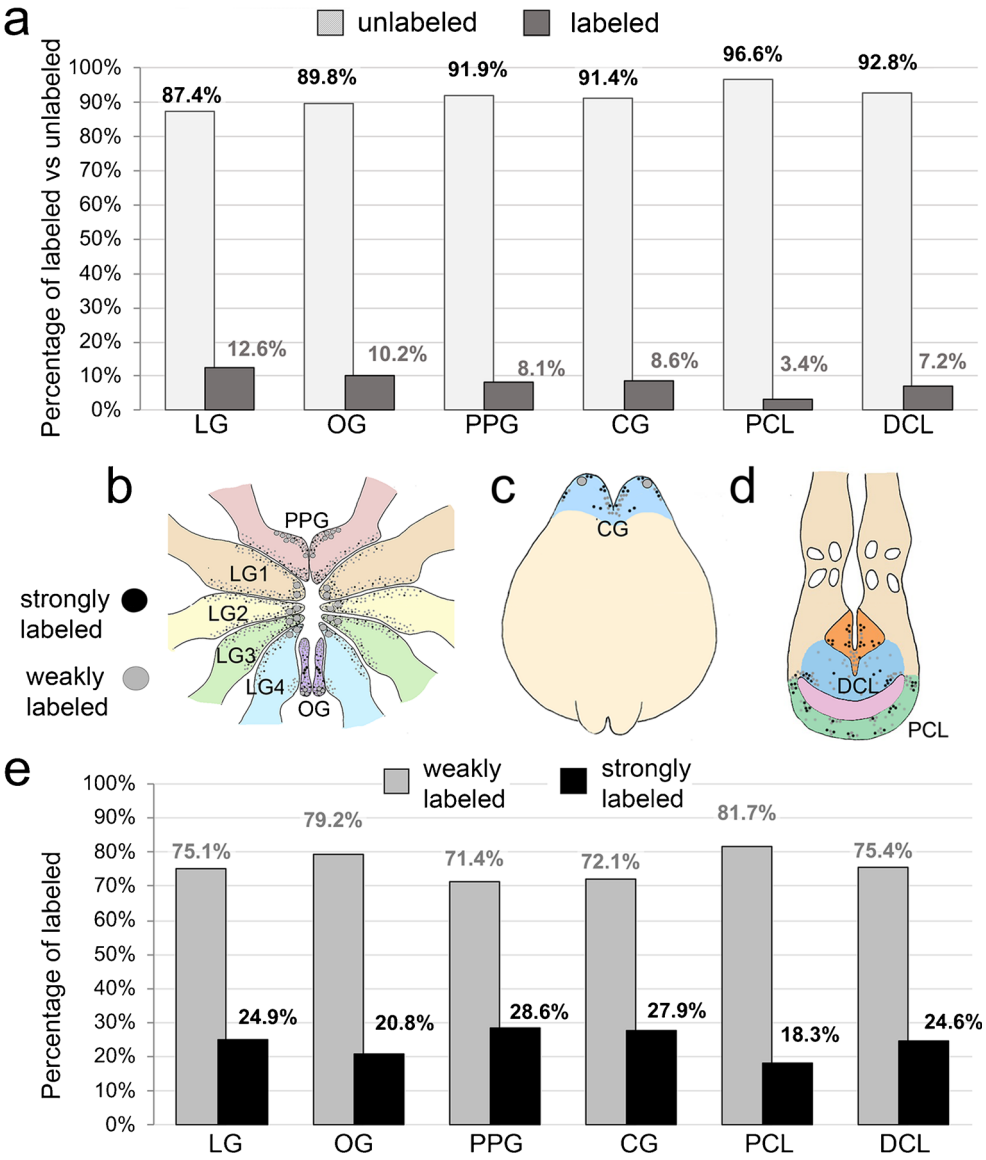

Fig. 2 **a** Histogram of FMRFa-LIR neurons (*dark gray columns*) versus unlabeled neurons (*light gray columns*). Throughout all ganglia, the majority of neurons appeared unlabeled. The largest percentage of labeled neurons was observed in the leg ganglia (*LG*; 12.6%) followed by the opisthosomal ganglia (*OG*, 10.2%), cheliceral ganglia (*CG*, 8.6%), pedipalpal ganglia (*PPG*, 8.1%), the dorsal cell layer (*DCL*, 7.2%) and the posterior cell layer (*PCL*, 3.4%). **b–d** Schematic drawings of the different ganglia and the locations of the strongly and weakly labeled neurons within the ganglia. **e** Histogram of the FMRFa-LIR neurons showing the percentage of strongly (*gray columns*) versus weakly (*black columns*) labeled neurons. The majority of neurons appeared weakly labeled. The highest percentage of strongly labeled neurons was observed in the pedipalpal ganglion (*PPG*, 28.6%), followed by the chelicer-al ganglion (*CG*, 27.9%), dorsal cell layer (*DCL*, 24.6%), leg ganglia (*LG*, 24.9%), opisthosomal ganglia (*OG*, 20.8%) and posterior cell layer (*PCL*, 18.3%)

FMRFa-LIR–labeled neurons compared to 96.6% ($n = 4338$) of unlabeled neurons (Fig. 2). The majority of immunoreactive neurons were weakly labeled (81.7%, $n = 125$) compared to strongly labeled cells (18.3%, $n = 28$). Most labeled neurons were arranged in mixed clusters of both labeling intensities and located in the lateral and medial areas throughout the ganglion (Fig. 7a–c). Among the strongly labeled neurons, 17% were small ($n = 26$) and only 1.3% ($n = 2$) were medium sized. No large neurons were observed in the PCL. The weakly labeled neuron population consisted of 77.1% ($n = 118$) of small and 4.6% ($n = 7$) of medium-sized neurons.

Dorsal cell layer (DCL) Located anterodorsally and dorsally to the central body, this ganglion contained 7.2% ($n = 708$) of FMRFa-LIR neurons with 92.8% of unlabeled neurons ($n = 9165$). Both weak and strong labeling patterns were observed, 75.4% ($n = 534$) and 24.6% ($n = 174$) respectively.

FMRFa-LIR in leg nerves and along leg muscle Our observations of weakly labeled putative motor neurons in leg ganglia suggest that this neuropeptide may be utilized as a neuromodulator in a subpopulation of neuromuscular junctions (see "Discussion"). We would therefore expect FMRFa-LIR axons within the main leg nerves projecting into the periphery and labeled terminals along leg muscle. Examination of the leg nerves revealed numerous FMRFa-LIR varicose fibers projecting into the periphery (Fig. 8a). Leg muscles showed an abundance of FMRFa-LIR varicosities along muscle fibers suggestive of neuromuscular junctions (Fig. 8b). Interestingly, this labeling pattern was localized to some muscle fibers, whereas other muscle fibers were unlabeled. Ultrastructural examination of neuromuscular junctions in muscle adjacent to mechanosensory neurons revealed the presence of diverse vesicle populations including large electron dense vesicles characteristic of neuropeptides (Fig. 8c, see "Discussion").

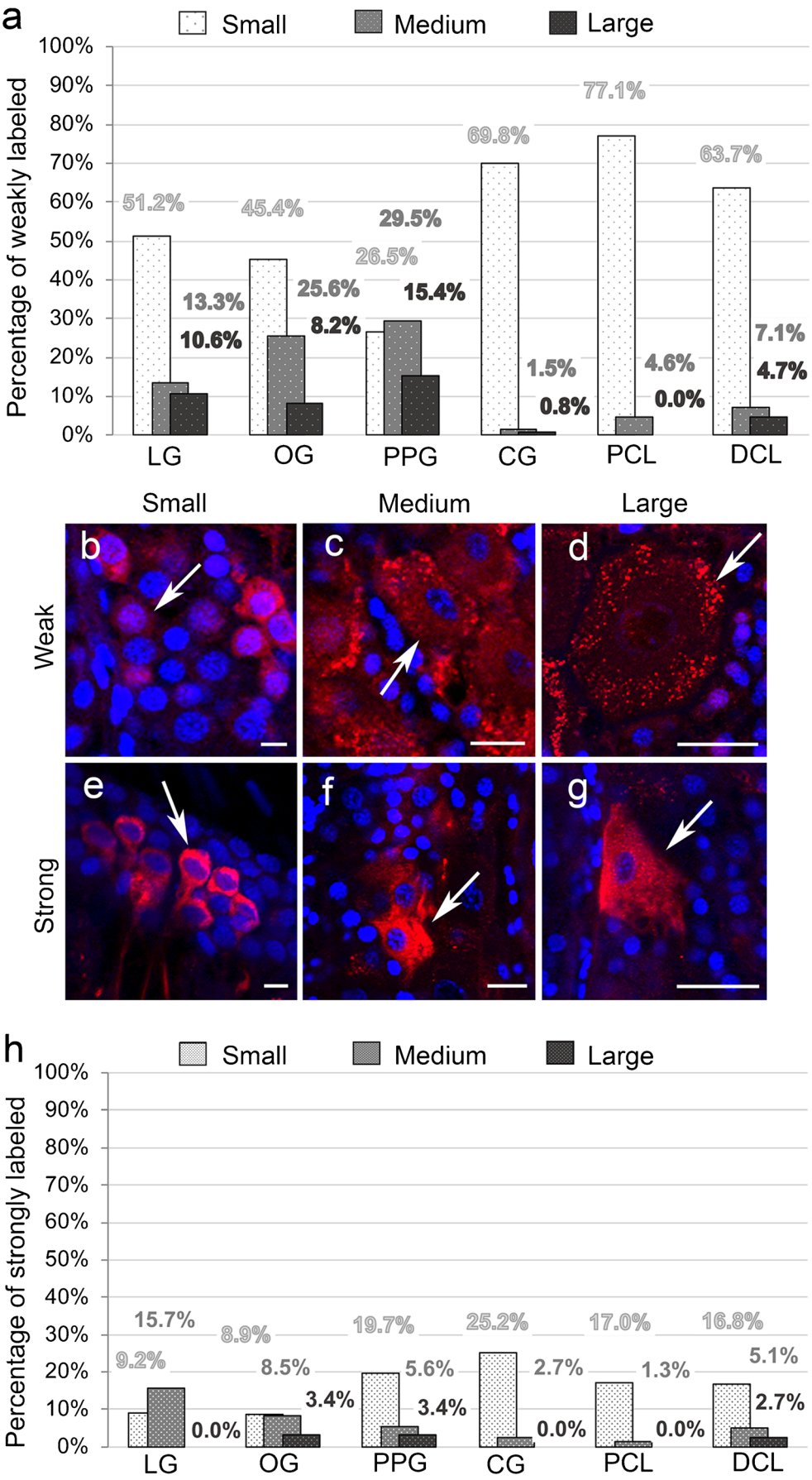

Fig. 3 Percentages of small, medium and large FMRFa-LIR neurons. **a** Histogram of the size distribution in weakly labeled neuron populations. **b–d** Examples of weakly labeled small (*arrow in* **b**), medium (*arrow in* **c**) and large (*arrow in* **d**) neurons. **e–g** Examples of strongly labeled small (*arrow in* **e**), medium (*arrow in* **f**) and large (*arrow in* **g**) neurons. **h** Histogram showing the size distribution in strongly labeled neuron populations. *Scale bars* (**a**, **e**) 10 μm; (**c**, **f**) 20 μm; (**d**, **g**) 50 μm

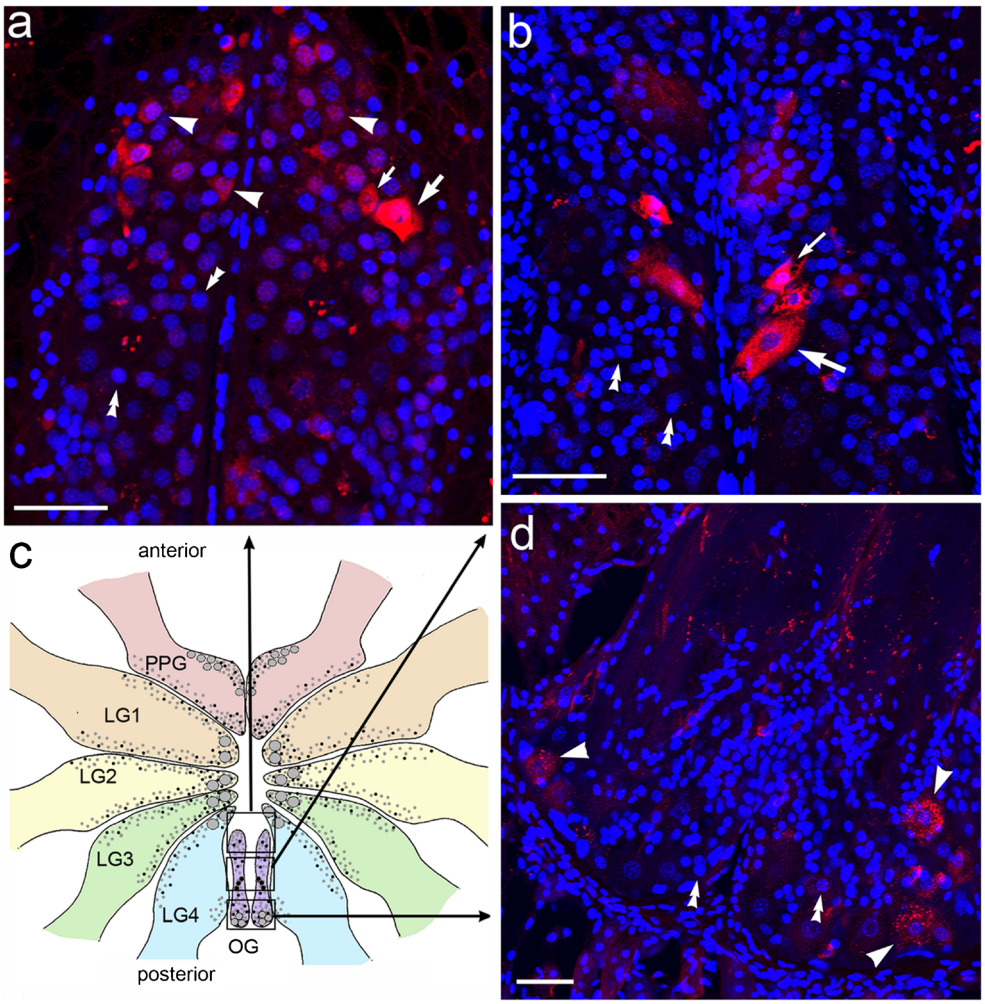

Fig. 4 Distribution of FMRFa-LIR neurons in the opisthosomal ganglion. Throughout the entire ganglia, weakly and strongly labeled neurons were observed. Characteristic neurons were consistently observed in the anterior, medial and posterior regions of the ganglia. **a** The majority of labeled neurons in the anterior region consisted of small weakly labeled (*arrowheads*) neurons. Some medium (*large arrow*) and small (*small arrow*) strongly labeled neurons were also observed. Hoechst Blue stain reveals numerous unlabeled neurons throughout the entire ganglion (*double arrowheads in* **a**, **b**, **d**). **b** Characteristic clusters of three strongly labeled neurons were observed in both hemispheres in the medial region of the ganglia (*arrows*). **c** Schematic drawing of the ganglia in the subesophageal ganglion. The outlined areas indicate the areas shown in **a**, **b** and **d**. **d** Weakly labeled, large neurons were observed in the posteriolateral areas of both hemispheres (*arrowheads*). *Scale bars* 50 μm

FMRFamide-glutamate double labeling FMRFa-LIR neurons in the PCL were located in areas where glutamate-like immunoreactive neurons have recently been described (Fabian-Fine et al. 2015). To investigate if some of these neurons display co-localization for both transmitters, we conducted double labeling for glutamate and FMRFamide. Our findings revealed that a subpopulation of weakly labeled FMRFa-LIR neurons also displayed strong glutamate-like immunoreactivity (glut-LIR). Interestingly, some of the strongly FMRFa-LIR neurons also showed strong glut-LIR (Fig. 9). We also observed FMRFa-LIR neurons that were negative for glutamate as well as Glut-LIR neurons that lacked FMRFa-LIR. Numerous neurons were void of immunolabeling for either transmitter.

Ultrastructural examination of presynaptic profiles in the CNS Ultrastructural investigation of presynaptic profiles throughout the CNS revealed a large variety of morphologically distinct presynaptic profiles characterized by diverse presynaptic vesicle populations (Fig. 9e). Whereas some terminals contained large populations of homogenous small (~ 20 nm in diameter) or large electron lucent vesicles (45–62 nm in diameter), others contained a large variety of mixed vesicle populations. The latter included small and large electron lucent vesicles that ranged between 20 and 62 nm and different types of electron dense vesicles such as large (80–100 nm in diameter) and small (~ 50 nm in diameter) electron dense vesicles, large dense core vesicles (~ 70 nm in diameter) and large medium-dense vesicles (~ 70–90 nm in diameter). Interestingly, many profiles containing mixed vesicle populations differed from each other with regard to vesicle type and number (Fig. 9e). These findings support our light microscopic observations of biochemically diverse neurons based on differences in their transmitter content and concentrations.

Discussion

In this study, we show the distribution of FaRPs throughout the nervous system of the Central American wandering spider *C. salei*. The distribution of FaRPs was described in the visual ganglia of the same model organism (Becherer and Schmid

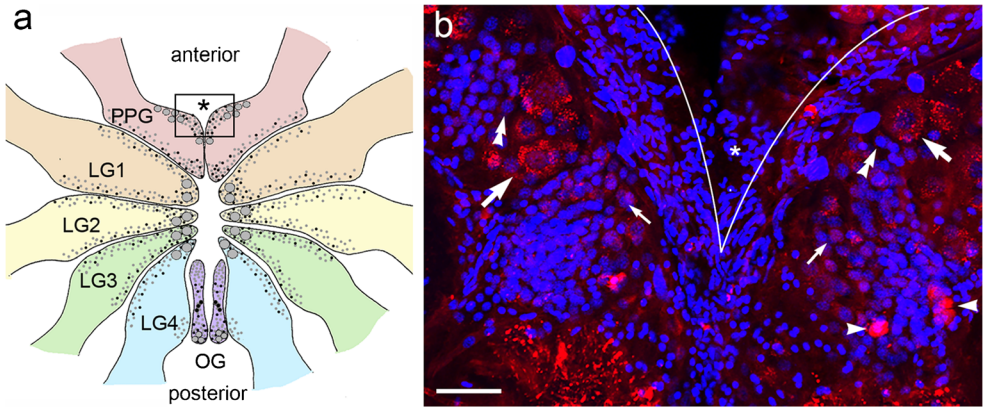

Fig. 5 FMRFa-LIR neurons in the pedipalpal ganglia. **a** Schematic drawing of the ganglia indicating the locations of the labeled neurons. The area indicated by the *inset* and *asterisk* corresponds to the area shown in **b**. *LG1–4*, leg ganglia 1–4; *PPG*, pedipalpal ganglia; *OG*, opisthosomal ganglia. **b** Most labeled neurons were weakly labeled, medium-sized neurons in the anterolateral region of the ganglia (*large arrows*). Numerous small, weakly labeled neurons were observed in the medial area of the ganglia (*small arrows*). *Arrowheads*, small, strongly labeled neurons. *Scale bar* 50 μm

1999) and the labeling patterns we observed throughout the visual system are largely consistent with those of this earlier study. Differences in labeling intensity in the PCL where Becherer and Schmid reported a stronger labeling signal can likely be attributed to differences in the detection methods for the secondary antibodies. Becherer and Schmid utilized an enzymatic peroxidase reaction, whereas we employed a fluorochrome-coupled secondary antibody. Enzymatic detection methods have been shown to be less localized as the reaction product may diffuse over short distances and thus appear more widely distributed compared to fluorochrome-coupled secondary antibodies that remain at the site of the epitope (Fabian-Fine et al. 1999a).

Weakly versus strongly labeled neurons

Strongly and weakly labeled neurons in *C. salei* have been reported previously for octopamine (Seyfarth et al. 1993), histamine (Fabian and Seyfarth 1997), GABA, glutamate (Fabian-Fine et al. 2015), acetylcholine (Fabian-Fine et al. 2017) and FaRPs (Becherer and Schmid 1999). One hypothesis for these differences in labeling intensities is the possible depletion of transmitter from neurons after strong stimulation. One observation that does not support this hypothesis is the fact that weakly labeled neurons appeared consistently weakly labeled throughout all evaluated brains and were not random as would have been expected in the case of activity-dependent depletion. This hypothesis is also inconsistent with the sites of transmitter release and synthesis for classic transmitters such as glutamate, GABA and acetylcholine. These fast-acting small molecule transmitters are usually released from presynaptic terminals and one would expect to see activity-dependent depletion of transmitters predominantly in presynaptic areas of the neuropil where these transmitters are released and recycled rather than the associated cell bodies. In the case of neuroactive peptides, this hypothesis could be valid since their synthesis takes place exclusively in the somata. The release of neuropeptides is not restricted to presynaptic sites but may also occur in the soma of the cells (Jan and Jan 1982; Boarder 1989; van den Pol 2012; Nusbaum et al. 2017).

A second hypothesis is that strongly labeled neurons represent projection neurons that send their axonal processes outside of their respective ganglia and form a network of numerous axon collaterals with abundant synaptic contacts throughout the CNS. The synthesis of neuropeptides is usually restricted to neuronal somata. Therefore, it is conceivable that projection neurons that form long axonal processes and numerous synaptic contacts synthesize larger amounts of neuropeptide and appear more brightly labeled compared to local circuit neurons with comparatively short axons and fewer synapses. The injection of fluorescent dyes into strongly and weakly labeled neurons to visualize their axonal projections may be useful to address this hypothesis.

A third hypothesis is that the weakly labeled neuroactive compounds act as a neuromodulator and thus occur at lower concentrations compared to the main transmitters utilized within the respective neurons. The fact that a majority of FMRFa-LIR neurons in our study are weakly labeled is consistent with this hypothesis and it is well known that modulatory neuropeptides act mainly on G-protein–mediated metabotropic receptors (Civelli 2012; Nusbaum et al. 2017). The required amount of transmitter to elicit a physiological response is small due to the amplification effect of G-protein–mediated second messenger cascades. Although in the case of FaRPs, direct action on FMRFamide-gated Na^+ channels has been described (Lingueglia et al. 1995), the receptors on which FaRPs act in the spider nervous system have not yet been identified.

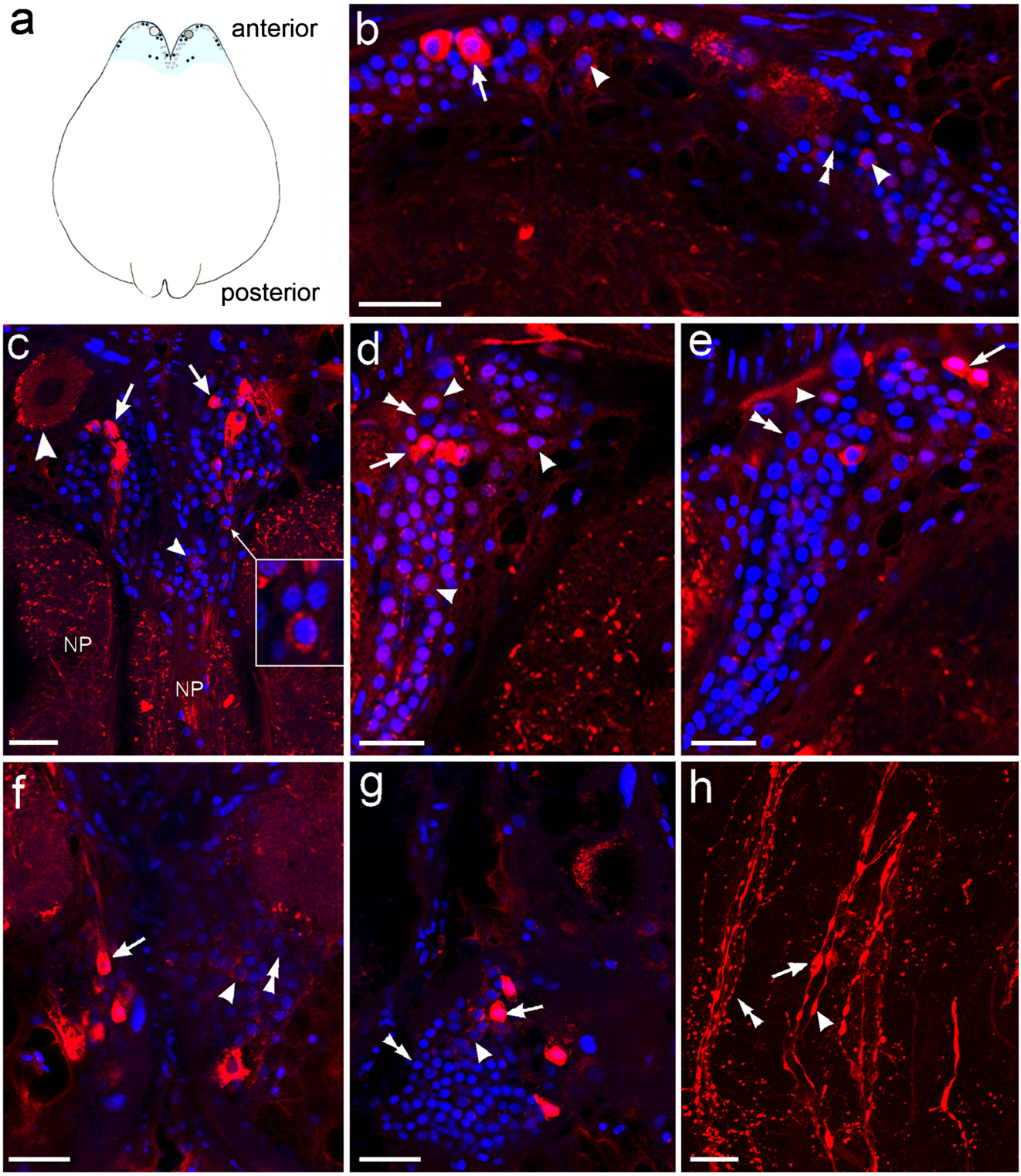

Fig. 6 FMRFa-LIR neurons in the cheliceral ganglia. **a** Schematic drawing of the ganglia indicating the location of the strongly (*black dots*) and weakly (*gray dots*) labeled neurons. **b** Anterior region of the left ganglion showing strongly labeled (*arrow*), weakly labeled (*arrowheads*) and unlabeled neurons (*double arrowhead*). **c–g** Most neurons are located in the anteromedial region of the ganglia. Hoechst Blue nuclear stain reveals that the majority of neurons appear unlabeled (*double arrowheads*). Numerous small, weakly labeled neurons can be observed throughout the area (*small arrowheads*). *Arrows*, strongly labeled small and medium-sized neurons. *Large arrowhead*, large weakly labeled motor neuron. *Inset in* **c**: higher zoom of a weakly labeled neuron; **h** numerous labeled varicose projections of different sizes were observed throughout the neuropil. *Double arrowheads*, small varicosities; *arrowhead*, medium varicosities; *arrow*, large varicosities. *Scale bars* (**b**, **d**, **e**) 50 μm; (**c**, **f**, **g**) 100 μm; (**h**) 5 μm

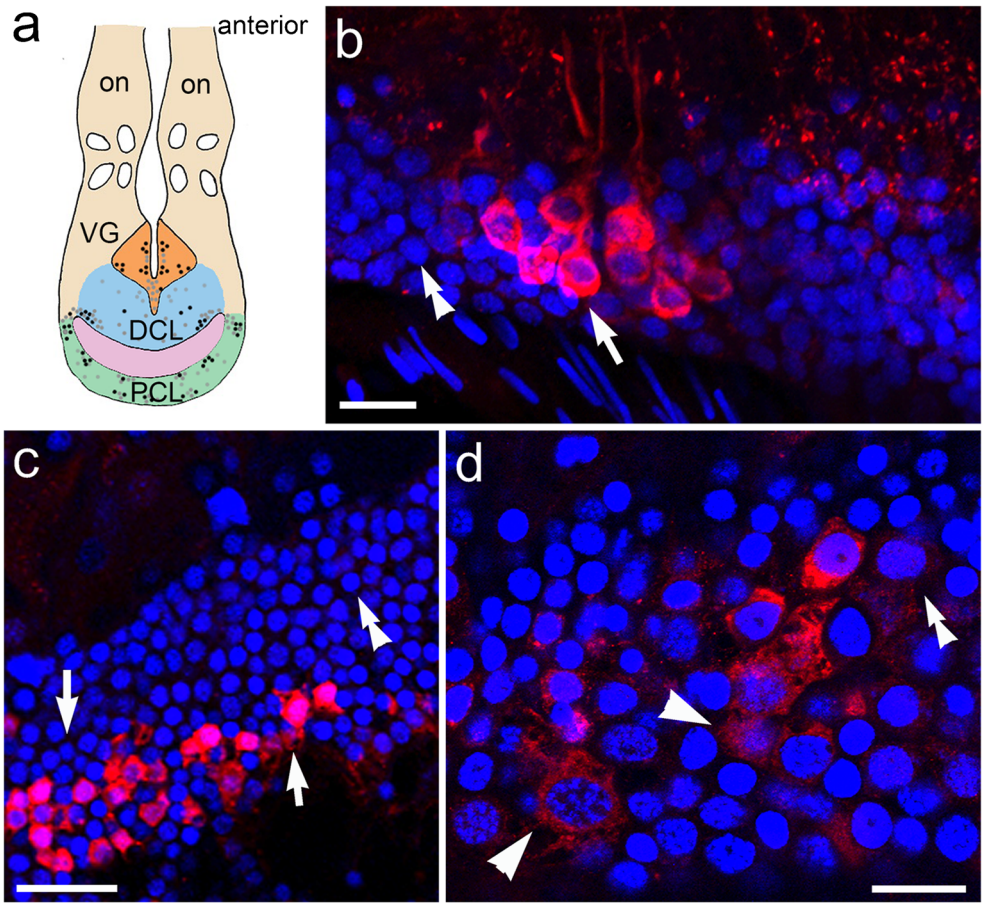

Fig. 7 FMRFa-LIR neurons in the posterior cell layer (*PCL*). **a** Schematic drawing of the visual area showing the location of immunolabeled neurons in the *PCL*, the dorsal cell layer (*DCL*) and visual ganglia (*VG*); *on*, optic nerves. **b–d** Clusters of strongly labeled (*arrows*) and weakly labeled neurons (*arrowheads*) can be observed throughout the PCL. The majority of neurons appeared unlabeled as visualized by Hoechst Blue nuclear stain (*double arrowheads*). Scale bars (**b**, **c**) 50 μm; (**d**) 10 μm

This third hypothesis is supported by our ultrastructural investigations revealing an unexpected variety of diverse presynaptic profiles with morphologically distinct vesicle populations. Although some transmitters are likely co-released from the same vesicles as demonstrated in the example of dopamine and GABA in the mammalian brain (Tritsch et al. 2012), in general, transmitters are released from morphologically distinct vesicle populations (Fabian-Fine et al. 2000; Salio et al. 2006; Merighi et al. 2011). The final answer to differences in the labeling intensities of FMRFa-LIR neurons may well be a mixture between the hypotheses discussed above.

Co-localization with glutamate and functional significance of FMRFamide

The distribution of FMRFa-LIR neurons in the CNS of *C. salei* revealed labeling in areas and neuron populations that have previously been described to show glut-LIR (Fabian-Fine et al. 2015). Double labeling for both transmitters revealed that there is indeed co-localization of both epitopes throughout the brain. Similar observations of FMRFamide/glutamate co-localization have been reported in cuttlefish (Loi and Tublitz 2000) where both transmitters have been shown to be present at chromatophore neuromuscular junctions initiating the expansion of dark brown chromatophores. Whereas glutamate initiated an instant and fast chromatophore expansion, the onset of FMRFamide-initiated expansion was delayed by up to 500 msec and longer lasting compared to the glutamate-initiated response. Similarly, effects have been described in abdominal extensor muscles of crayfish, where FaRPs have been shown to increase the amplitude of excitatory junctional potentials in a dose-dependent manner (Skerrett et al. 1995). The physiological effects of FaRPs however do not seem to be limited to the slow onset of activation but may be more diverse. For example in the nematode *Caenorhabditis elegans*, the upregulation of FaRPs has been observed during the stress-induced entry of larval stages into dauerlarvae, which alter physiological and behavioral patterns until environmental conditions are more favorable for survival (Lee et al. 2017). We are currently conducting a detailed characterization of the co-localization of glutamate and FaRPs throughout the spider nervous system. In future experiments, functional studies are required to investigate the effect of FaRPs on the leg muscle in *C. salei* and mechanosensory neurons. As discussed in the following two paragraphs, of particular interest are the projection pathways of the glutamate/FMRFa-LIR neurons.

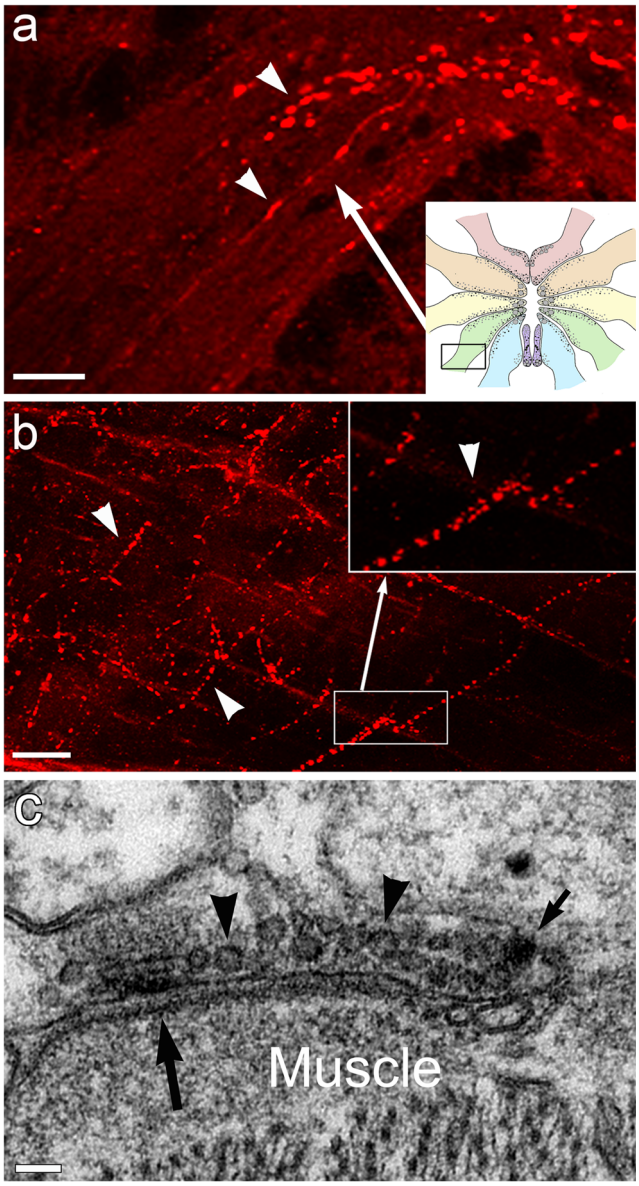

Fig. 8 **a**, **b** FMRFa-LIR varicose neuronal processes projecting into the leg nerves (*arrowheads in* **a**) and along leg muscle (*arrowheads in* **b**). **c** Electron micrograph of a neuromuscular synapse (*large arrow*) containing electron lucent (*arrowheads*) and peripherally located electron dense (*arrow*) vesicles. *Inset in* **a**: area in the spider central nervous system shown in **a**. *Inset in* **b**: higher zoom of varicose projections shown in the corresponding inset. *Scale bars* (**a**) 15 μm; (**b**) 18 μm; (**c**) 30 nm

Immunolabeled neuron types and their central and peripheral projection patterns

In an anatomical study of the spider central nervous system, Babu and Barth (1984) classified large and medium-sized neurons as motor neurons, interneurons, or neurosecretory nerve cells. The larger neurons often send their axonal processes to more distant receptive partners such as leg muscles, adjacent ganglia and projection pathways, or peripherally located sensory neurons. Some neurons project from the dorsally located visual area to the ventrally located leg ganglia as demonstrated by Schmid and Dunker (1993) in the example of histamine-like immunoreactive neurons. Small neurons are often local circuit neurons that communicate information within their respective ganglia. The different types of FMRFa-LIR immunoreactive axonal projections in neuropil areas provide evidence that a subpopulation of small neurons may also send their axonal projections over longer distances, parallel to large and medium axonal profiles. Previous studies of efferent projections onto sensory neurons in slit sense organs have shown that the small axonal profiles form small synaptic contacts onto the medium and large neuron profiles and vice versa, creating an intricate network of efferent control onto sensory neurons (Fabian-Fine et al. 1999b, 2000). The presence of FMRFa-LIR efferent projections along mechanosensory neurons has previously been described (Fabian-Fine et al. 2017). It is unclear where these efferent neurons originate and whether efferent fibers that run in parallel originate in the same ganglion or from different ganglia within the CNS. This information is of critical importance to understand how sensory neurons are controlled by efferent neurons. As mentioned above, intracellular injection of fluorescent dyes into FMRFa-LIR neurons may be a suitable approach to answer this question.

Neurochemical diversity of neurons and their implications for behavioral circuits

Our observations in conjunction with previous observations of biochemically diverse neurons in the CNS of *C. salei* (see above) indicate that the spider CNS contains a large variety of biochemically diverse neuron populations with many neurons co-transmitting two or more neuroactive compounds. These observations are not unique to *C. salei*, in fact there is evidence, especially from serial section microscopy, in both vertebrate and invertebrate model systems suggesting that most, if not all, neurons express more than one transmitter type (Church and Lloyd 1991; Trudeau 2004). Studies in *Drosophila melanogaster* have revealed an astounding variety of biochemically diverse neurons containing mixtures of two or more (1) fast-acting small molecule transmitters, (2) small molecule transmitters and neuropeptides and (3) neuroactive peptides (Kolodziejczyk et al. 2008; Croset et al. 2017; Nässel 2018). There is an increasing body of literature on transmitter co-expression. The functional implications of this phenomenon are suggestive of an astoundingly rich and complex repertoire of mechanosensory perception in spiders, which likely contributed to the evolutionary success of these arthropods. It also highlights the importance of the systematic morphological, biochemical and functional characterization of this exceptionally suitable model system to gain a better understanding of signal transduction in mechanosensory organs.

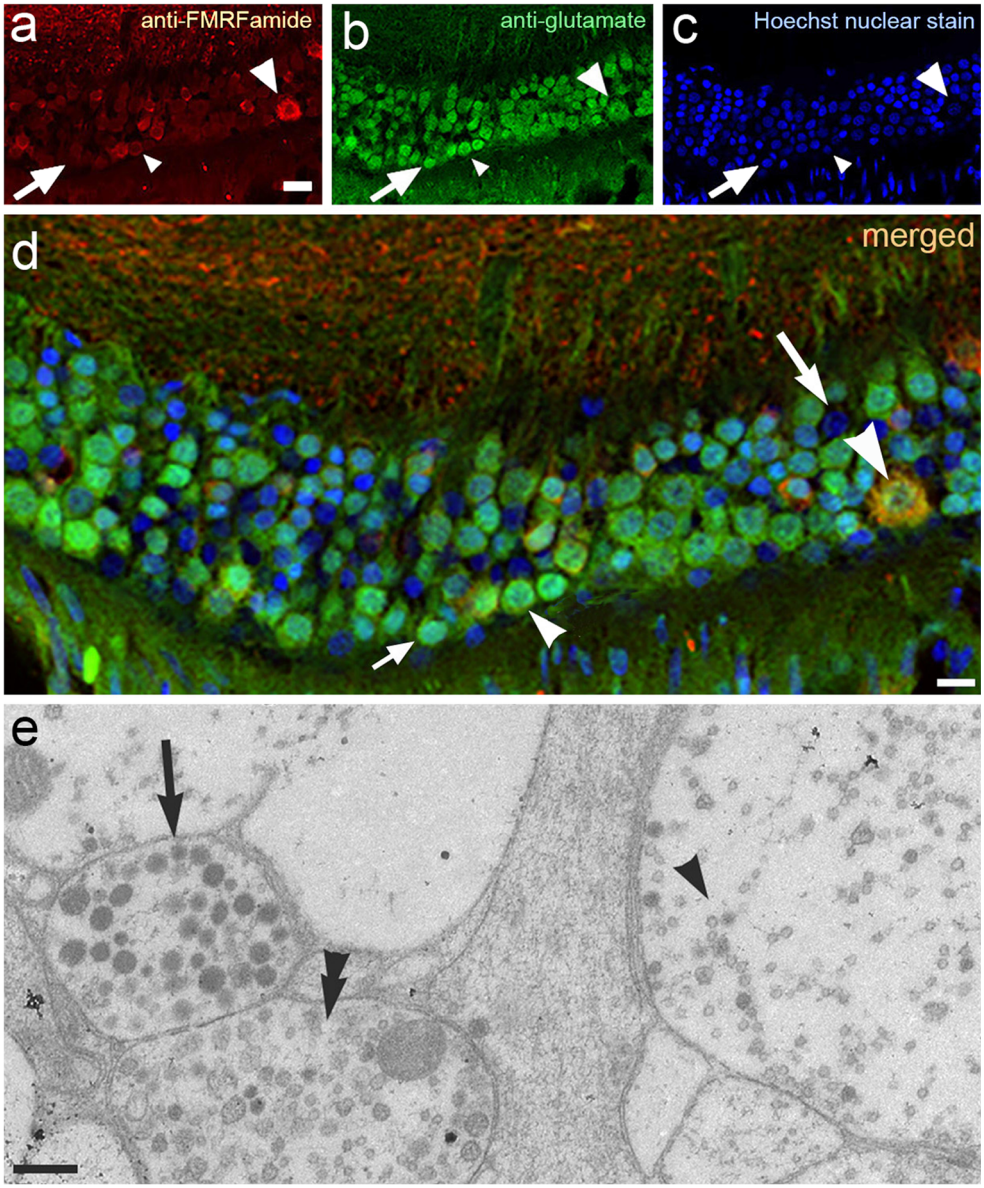

Fig. 9 Biochemically diverse neuron populations in the CNS. **a–d** FMRFamide (*red*) and glutamate (*green*) double labeling in the posterior cell layer show at least four biochemically diverse neuron types. *Large arrowheads*, neuron with strong labeling intensity for both FMRFa-LIR and glutamate-LIR. *Small arrowhead*, neuron with weak FMRFa-LIR and strong glutamate immunoreactivity. *Small arrows in* **a–d**: glutamate-LIR neuron that is negative for FMRFa-LIR. *Large arrow in* **d**: unlabeled neuron in which only the Hoechst Blue–stained nucleus is visible. **e** Electron micrograph showing three vesicle-laden neuronal profiles with morphologically diverse vesicle populations (*arrow*, *arrowhead*, *double arrowheads*). *Scale bars* (**a–d**) 20 μm; (**e**) 210 nm

Acknowledgements Confocal imaging was performed at the University of Vermont Microscopy Imaging Center. The authors thank Dr. Douglas Taatjes, Nicole Bouffard and Nicole Bishop for continued support with confocal microscopy. We thank Duy Pham of Colchester High School/Vermont for the artwork in Fig. 1(a). Its contents are solely the responsibility of the authors and do not necessarily represent the official views of NIGMS or NIH.

Funding information The Zeiss 510 META laser scanning confocal microscope was supported by NIH Award Number 1S10RR019246 from the National Center for Research Resources. The Alden Foundation supported the purchase of essential equipment for the SMC Biology Department. KG and BF received generous research stipends from Mr. Michael J. Cunniff and Dr. Robert F. Tobin. This research was supported by an Institutional Development Award (IDeA) from the National Institute of General Medical Sciences of the National Institutes of Health under grant number P20GM103449 (RF-F, BF, ET, KC, CA, KG and AJ). Further support was received in the form of a research stipend from The John C Hartnett fund to NG.

References

Babu KS, Barth FG (1984) Neuroanatomy of the central nervous system of the wandering spider, *Cupiennius salei* (Arachnida, Araneida). Zoomorphol 104:344–359

Barth FG, Libera W (1970) Ein Atlas der Spaltsinnesorgane von *Cupiennius salei* Keys. Chelicerata (Araneae). Z Morph Ökol Tiere 68:343–369

Becherer C, Schmid A (1999) Distribution of ɣ-aminobutyruc acid-, proctolin-, *Periplaneta* hypertrehalosaemic hormone- and FMRF-amide-like immunoreactiviy in the visual ganglia of the spider *Cupiennius salei* Keys. Comp Biochem Physiol 122:267–275

Boarder MR (1989) Presynaptic aspects of cotransmission: relationship between vesicles and neurotransmitters. J Neurochem 53:1–11

Church PJ, Lloyd PE (1991) Expression of diverse neuropeptide cotransmitters by identified motor neurons in Aplysia. J Neurosci 11:618–625

Civelli O (2012) Orphan GPCRs and neuromodulation. Neuron 76:12–21

Croset, V., Treiber, C. D., and Waddell, S. (2017). Cellular diversity in the Drosophila midbrain revealed by single-cell transcriptomics. bioRxiv. https://doi.org/10.1101/237818 [preprint]. Now in eLife

Fabian R, Seyfarth EA (1997) Acetylcholine and histamine are transmitter candidates in identifiable mechanosensitive neurons of the spider Cupiennius salei: an immunocytochemical study. Cell Tissue Res 287:413–423

Fabian-Fine R, Anderson CM, Roush MA, Johnson JAG, Liu H, French AS, Torkkeli PH (2017) The distribution of cholinergic neurons and their co-localization with FMRFamide, in central and peripheral neurons of the spider Cupiennius salei. Cell Tissue Res 370:71–88

Fabian-Fine R, Volknandt W, Seyfarth E (1999a) Peripheral synapses at identifiable mechanosensory neurons in the spider Cupiennius salei: synapsin-like immunoreactivity. Cell Tissue Res 295:13–19

Fabian-Fine R, Hoger U, Seyfarth EA, Meinertzhagen IA (1999b) Peripheral synapses at identified mechanosensory neurons in spiders: three-dimensional reconstruction and GABA immunocytochemistry. J Neurosci 19:298–310

Fabian-Fine R, Meinertzhagen IA, Seyfarth EA (2000) Organization of efferent peripheral synapses at mechanosensory neurons in spiders. J Comp Neurol 420:195–210

Fabian-Fine R, Meisner S, Torkkeli PH, Meinertzhagen IA (2015) Co-localization of gamma-aminobutyric acid and glutamate in neurons of the spider central nervous system. Cell Tissue Res 362:461–479

Foelix RF, Chu-Wang IW (1973) The morphology of spider sensilla. I. Mechanoreceptors. Tissue & Cell 5:451–460

Jan LY, Jan YN (1982) Peptidergic transmission in sympathetic ganglia of the frog. J Physiol 327:219–246

Kolodziejczyk A, Sun X, Meinertzhagen IA, Nässel DR (2008) Glutamate, GABA and acetylcholine signaling components in the lamina of the Drosophila visual system. PLoS One 3:e2110. https://doi.org/10.1371/journal.pone.0002110

Lingueglia E, Champigny G, Lazdunski M, Barbry P (1995) Cloning of the amiloride-sensitive FMRFamide peptide-gated sodium channel. Nature 378:730–733

Lee JS, Shih PY, Schaedel ON, Quintero-Cadena P, Rogers AK, Sternberg PW (2017) FMRFamide-like peptides expand the behavioral repertoire of a densely connected nervous system. Proc Natl Acad Sci U S A 114:E10726–E10735

Liu X, Porteous R, d'Anglemont de Tassigny X, Colledge WH, Millar R, Petersen SL, Herbison AE (2011) Frequency-dependent recruitment of fast amino acid and slow neuropeptide neurotransmitter release controls gonadotropin-releasing hormone neuron excitability. J Neurosci 31:2421–2430

Loi PK, Tublitz NJ (2000) Roles of glutamate and FMRFamide-related peptides at the chromatophore neuromuscular junction in the cuttlefish, *Sepia officinalis*. J Comp Neurol 420:499–511

Merighi A, Salio C, Ferrini F, Lossi L (2011) Neuromodulatory function of neuropeptides in the normal CNS. J Chem Neuroanat 42:276–287

Nässel DR (2018) Substrates for neuronal cotransmission with neuropeptides and small molecule neurotransmitters in Drosophila. Front Cell Neurosci 12(83)

Nusbaum MP, Blitz DM, Marder E (2017) Functional consequences of neuropeptide and small-molecule co-transmission. Nat Rev Neurosci 18:389–403

Panek I, French AS, Seyfarth EA, Sekizawa S, Torkkeli PH (2002) Peripheral GABAergic inhibition of spider mechanosensory afferents. Eur J Neurosci 16:96–104

Panek I, Torkkeli PH (2005) Inhibitory glutamate receptors in spider peripheral mechanosensory neurons. Eur J Neurosci 22:636–646

Pfeiffer K, Panek I, Hoger U, French AS, Torkkeli PH (2009) Random stimulation of spider mechanosensory neurons reveals long-lasting excitation by GABA and muscimol. J Neurophysiol 101:54–66

Rabbitt RD, Brownell WE (2011) Efferent modulation of hair cell function. Current Opinion Otolaryngology Head Neck Surgery 19:376–381

Salio C, Lossi L, Ferrini F, Merighi A (2006) Neuropeptides as synaptic transmitters. Cell Tissue Res 326:583–598

Schmid A, Dunker M (1993) Histamine immunoreactivity in the central nervous system of the spider Cupiennius salei. Cell Tiss Res 273:533–545

Schrott-Fischer A, Kammen-Jolly K, Scholtz A, Rask-Andersen H, Glueckert R, Eybalin M (2007) Efferent neurotransmitters in the human cochlea and vestibule. Acta Otolaryngol 127:13–19

Schwarzer C, Sperk G (1995) Hippocampal granule cells express glutamic acid decarboxylase-67 after limbic seizures in the rat. Neuroscience 69:705–709

Seyfarth EA, Hammer K, Sporhase-Eichmann U, Horner M, Vullings HG (1993) Octopamine immunoreactive neurons in the fused central nervous system of spiders. Brain Res 611:197–206

Seyfarth EA, French AS (1994) Intracellular characterization of identified sensory cells in a new spider mechanoreceptor preparation. J Neurophysiol 71:1422–1427

Skerrett M, Peaire A, Quigley P, Mercier A (1995) Physiological effects of two FMRFamide-related peptides from the crayfish Procambarus clarkii. J Exp Biol 198:109–116

Sloviter RS, Dichter MA, Rachinsky TL, Dean E, Goodman JH, Sollas AL, Martin DL (1996) Basal expression and induction of glutamate decarboxylase and GABA in excitatory granule cells of the rat and monkey hippocampal dentate gyrus. J Comp Neurol 373:593–618

Suggs JM, Jones TH, Murphree SC, Hillyer JF (2016) CCAP and FMRFamide-like peptides accelerate the contraction rate of the antennal accessory pulsatile organs (auxiliary hearts) of mosquitoes. J Exp Biol 219:2388–2395

Tritsch NX, Ding JB, Sabatini BL (2012) Dopaminergic neurons inhibit striatal output through non-canonical release of GABA. Nature 490:262–266

Trudeau LE (2004) Glutamate co-transmission as an emerging concept in monoamine neuron function. J Psychiatry Neuroscience : JPN 29:296–310

van den Pol AN (2012) Neuropeptide transmission in brain circuits. Neuron 76:98–115

Whim MD, Lloyd PE (1989) Frequency-dependent release of peptide cotransmitters from identified cholinergic motor neurons in Aplysia. Proc Natl Acad Sci U S A 86:9034–9038

Widmer A, Hoger U, Meisner S, French AS, Torkkeli PH (2005) Spider peripheral mechanosensory neurons are directly innervated and modulated by octopaminergic efferents. J Neurosci 25:1588–1598